ENERGY CONFINEMENT AND PROFILE CONSISTENCY IN TFTR

R.J. GOLDSTON, V. ARUNASALAM, M.G. BELL, M. BITTER, W.R. BLANCHARD, N.L BRETZ, R. BUDNY, C.E. BUSH[1], J.D. CALLEN[2], S.A. COHEN, S.K. COMBS[1], S.L. DAVIS, D.L. DIMOCK, H.F. DYLLA, P.C. EFTHIMION, L.C. EMERSON[1], A.C. ENGLAND[1], H.P. EUBANK, R.J. FONCK, E. FREDRICKSON, H.P FURTH, G. GAMMEL, B. GREK, L.R. GRISHAM, G. HAMMETT, R.J., HAWRYLUK, W.W. HEIDBRINK[3], D.B. HEIFETZ, H.W. HENDEL[4], K.W. HILL, E. HINNOV, S. HIROE[1], H. HSUAN, R.A. HULSE, K.P. JAEHNIG, D. JASSBY, F.C. JOBES, D.W. JOHNSON, L.C. JOHNSON, R. KAITA, R. KAMPERSCHROER, S.M. KAYE, S.J. KILPATRICK, R.J. KNIZE, H. KUGEL, P.H. LaMARCHE, B. LeBLANC, R. LITTLE, C.H. MA[1], D.M. MANOS, D.K. MANSFIELD, R.T. McCANN, M.P. McCARTHY, D.C. McCUNE, K. McGUIRE, D.H. McNEILL, D.M. MEADE, S.S. MEDLEY, D.R. MIKKELSEN, S.L. MILORA[1], W. MORRIS[5], D. MUELLER, V. MUKHOVATOV[6], E.B. NIESCHMIDT[7], J. O'ROURKE[8], D.K. OWENS, H. PARK, N. POMPHREY, B. PRICHARD, A.T. RAMSEY, M.H. REDI, A.L. ROQUEMORE, P.H. RUTHERFORD, N.R. SAUTHOFF, G. SCHILLING, J. SCHIVELL, G.L. SCHMIDT, S.D. SCOTT, S. SESNIC, J.C. SINNIS, F.J. STAUFFER[9], B.C. STRATTON, G.D. TAIT, G. TAYLOR, J.R. TIMBERLAKE, H.H. TOWNER, M. ULRICKSON, V. VERSHKOV[6], S. VON GOELER, F. WAGNER[10], R. WIELAND, J.B. WILGEN[1], M. WILLIAMS, K.L. WONG, S. YOSHIKAWA, R. YOSHINO[11], K.M. YOUNG, M.C. ZARNSTORFF, V.S. ZAVERYAEV[6], S.J. ZWEBEN
Princeton Plasma Physics Laboratory,
Princeton University,
Princeton, New Jersey,
United States of America

[1] Oak Ridge National Laboratory, Oak Ridge, TN, USA.
[2] University of Wisconsin, Madison, WI, USA.
[3] GA Technologies Inc., San Diego, CA, USA.
[4] RCA David Sarnoff Research Center, Princeton, NJ, USA.
[5] Balliol College, University of Oxford, Oxford, UK.
[6] Kurchatov Institute of Atomic Energy, Moscow, USSR.
[7] EG&G Idaho, Inc., Idaho Falls, ID, USA.
[8] JET Joint Undertaking, Abingdon, Oxfordshire, UK.
[9] University of Maryland, College Park, MD, USA.
[10] Max-Planck-Institut für Plasmaphysik, Garching, Fed. Rep. Germany.
[11] JAERI, Naka-machi, Naka-gun, Ibaraki-ken, Japan.

Abstract

ENERGY CONFINEMENT AND PROFILE CONSISTENCY IN TFTR.

A new regime of enhanced energy confinement has been observed on TFTR with neutral beam injection at low plasma current. It is characterized by extremely peaked electron density profiles and broad electron temperature profiles. The electron temperature profile shapes violate the concept of profile consistency in which $\langle T_{e0}/T_e \rangle_v$ is assumed to be a tightly constrained function of q_a, but they are in good agreement with a form of profile consistency based on examining the temperature profile shape outside of the plasma core. The enhanced confinement regime is only obtained with a highly degassed limiter; in discharges with gas filled limiters convective losses are calculated to dominate the edge electron power balance. Consistent with the constraint of profile consistency, global confinement is degraded in these cases. The best heating results in the enhanced confinement regime are obtained with nearly balanced co- and counter-injection. Much of the difference between balanced and co-only injection can be explained on the basis of classically predicted effects associated with plasma rotation.

1. Introduction

A new regime of enhanced energy confinement has been observed on TFTR with neutral beam injection at low plasma current. It is characterized by extremely peaked electron density profiles and broad electron temperature profiles. The best heating results in this regime are obtained with nearly balanced co and counter injection. The properties of these discharges (referred to as "supershots") raise questions about some of the recently achieved understanding of tokamak auxiliary heating physics - electron temperature profile consistency, and the lack of importance of toroidal rotation, among others. In this paper we discuss the implications of our results in these areas. We begin (Sec. 2) by putting the electron stored energy results in this new regime into the context of previous scaling laws and TFTR data, showing that these discharges exhibit enhanced electron energy confinement as well as the high total stored energy and ion temperature discussed in [1]. Next (Sec. 3) we study the electron temperature profile shapes of these enhanced confinement discharges, in comparison with L-Mode and ohmically heated profiles on TFTR. In Section 4 we address issues connected with the electron density profile shape. In Section 5 we discuss the role of rotation and balanced versus unbalanced injection.

2. Stored Electron Energy in Supershots

Figure 1 shows the electron energy content from a series of scans of neutral beam power at I_p = 0.9, 1.4, and 2.2 MA, with the plasma resting on the inner-wall carbon limiter. The scans at higher current were performed without any special limiter degassing procedures. They show typical L-Mode behavior: the stored energy reaches equilibrium during the beam pulse, and broad density profiles are observed. The 0.9 MA data were taken after extensive degassing with low density He discharges [2]; they

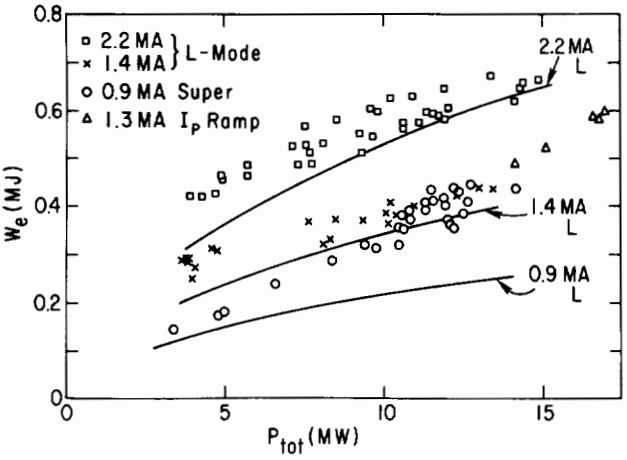

FIG. 1. Electron stored energy versus total heating power for 2.2 MA and 1.4 MA L-mode discharges and for 0.9 MA enhanced confinement discharges. Also shown are enhanced confinement discharges at 1.3 MA achieved by ramping the plasma current up from 0.9 MA during the injection pulse. The curves represent 0.4 × w^L_{tot}, where w^L_{tot} is the L-mode scaling predication [4] for total stored energy (see text).

generally show rising stored energy throughout the beam pulse, and at higher powers they exhibit strongly centrally peaked density profiles. Shots with severe MHD activity [3] which caused the stored energy and neutron flux to fall at the end of the pulse have been excluded from this data set. The higher current data sets have been constrained to $0.25 < P_{co}/P_{inj} < 0.75$, while the 0.9 MA data set has been constrained to $0.35 < P_{co}/P_{inj} < 0.65$, in order to minimize the effects of unbalanced injection, which are greatest in the low-current region [1]. The current of 0.9 MA was selected because at lower plasma currents (I_p = 0.7-0.8 MA) high power operation is prevented by severe MHD activity and disruptions, while the data set at higher currents (I_p = 1 - 1.1 MA) and P_{inj} less than 10 MW is very limited. Up to 17 MW of neutral beam power has been injected into discharges with an initial plasma current of 0.9 MA, without inducing strong MHD oscillations or disruptions, by ramping the plasma current up to 1.3 MA during the 0.5 sec beam pulse. Due to our present beam configuration, at these high powers $P_{co}/P_{inj} > 0.70$, which has been observed to result in significantly reduced heating compared to balanced injection at lower powers. Also plotted on this figure is the prediction of L-Mode scaling [4] (for $H^0 \rightarrow D^+$ injection) where the prediction of the scaling law for electron energy has been taken to be 0.4 times the prediction for total stored energy, since this ratio is characteristic of high power TFTR results in the standard regime. While the higher current results approach the L-Mode prediction at high powers, the 0.9 MA

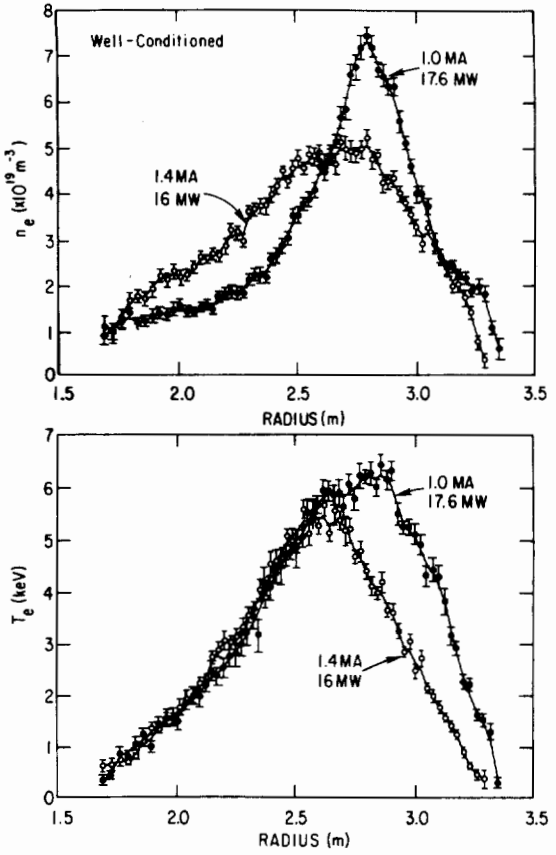

FIG. 2. Electron density and temperature profiles for a 1.0 MA enhanced confinement discharge (solid points) and for a 1.4 MA L-mode discharge (open points). For the enhanced confinement discharge: W_e = 0.52 MJ. For the L-mode discharge: W_e = 0.47 MJ. P_{co}/P_{inj} = 0.7 for both.

supershot results clearly diverge from it. The stored electron energy of the 1.3 MA current-ramp supershots is remarkably close to the standard regime 2.2 MA data. The magnetically-measured total stored energies of enhanced confinement discharges show even more of a gain over standard L-Mode discharges. The total stored energy of 0.9 MA supershots equals that of 2.2 MA standard regime discharges at powers in the range of 11 MW. The fact that kinetic stored energy calculations agree well with the diamagnetic measurement results (± 5% in the 0.9 MA data set shown here) indicates that the thermal and beam ions gain in stored energy as expected due to the high electron temperatures and peaked density profiles provided by supershots.

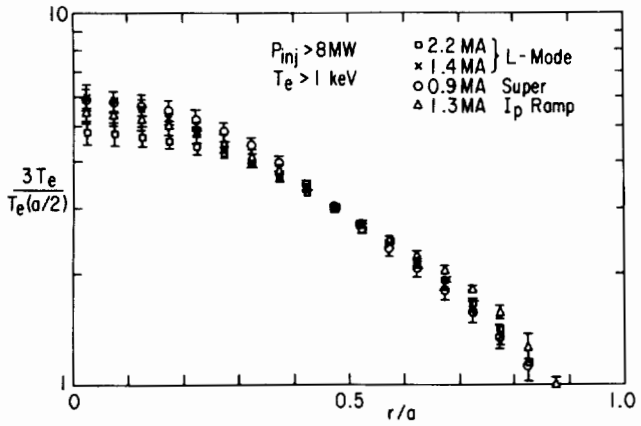

FIG. 3. Electron temperature profile shape normalized to r = a/2 for the data sets of Fig. 1. The factor of three is applied in order to centre the mid-radius on a single decade scale. The error bars represent the root mean square (RMS) variation of the data.

3. Electron Temperature Profile Consistency

Figure 2 shows an overlay of the Thomson scattering measurements of $T_e(R)$ and $n_e(R)$ from a supershot with I_p = 1 MA, B_T = 5T, and from a 1.4 MA discharge at the same toroidal field. Both discharges had a well-degassed limiter, but in the 1.4 MA case β_p nonetheless saturated after 0.3 sec into the beam pulse, and the density profile did not gain the peaked shape characteristic of the enhanced confinement mode. These results, and others like them, violate the concept of electron temperature profile consistency in which $T_e(0)/\langle T_e \rangle_v$ is taken as the measure of profile shape and is postulated to be a tightly-defined, monotonically rising function of q_a. This measure of profile shape is, however, already suspect as an indicator of microscopic transport mechanisms, since it can be largely enforced by sawtooth oscillations [4,5], if χ_e is sufficiently peaked to the outside of the discharge. On TFTR it has been previously observed [6] that the detailed electron temperature profile shape, outside of the core of the plasma and in the region where T_e > 1 keV, shows a remarkable constancy, independent of heating power - and most surprisingly - independent of q_a. Figure 3 shows electron temperature profile shapes normalized at r = a/2 for the points with P_{tot} > 8 MW in the power scans of Fig. 1. The electron temperatures measured by Thomson scattering have been mapped to flux surfaces, and plotted as a function of midplane minor radius. The two-sided electron temperature measurement ensures that this process unambiguously corrects for the strong Shafranov shift observed in the low current, enhanced confinement regime.

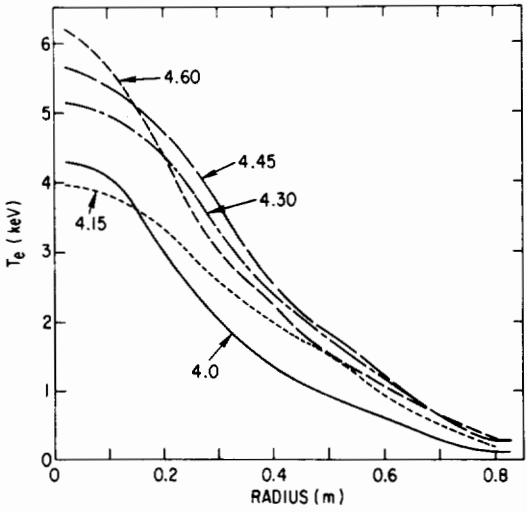

FIG. 4. Time evolution of $T_e(r)$ from Thomson scattering, mapped to time dependent magnetic flux surfaces for 9.5 MW balanced injection into a 0.8 MA discharge, in enhanced confinement regime. Neutral beam injection heating from t = 4.0 s to 4.5 s.

The error bars indicate the R.M.S. variation of the data. The 0.9 MA supershot temperature profiles line up with the L-Mode profiles in the region outside of a/3. The few current ramp shots show an approximately 10% higher $T_e(0.8a)/T_e(0.4a)$ than the others. Whether this is significant is difficult to say. Ohmic discharges at these same currents overlay well with this data, although in their case the selection for T_e > 1keV reduces the amount of data available outside 0.7a. In general it is found here, as in the data of [6], that the temperature profiles tend to fall off more steeply in the region where T_e < 1 keV. This suggests that processes such as impurity radiation, charge-exchange, and convection, which are likely to be more important at the colder edge of the plasma, control T_e in this region and help set the amplitude for the overall electron temperature profile.

While the mid-region temperature profiles are consistent with previous results in TFTR, the central region of the temperature profile in high-power enhanced confinement discharges is truncated in comparison with high-q ohmic target discharges (t = 4.45 sec versus t = 4.0 sec in Fig. 4), despite the absence of regular sawtooth oscillations during the heating phase [3]. One hypothesis to explain this effect is that the neutral beams provide a large source of cold electrons in the core region. Time-dependent transport analysis of balanced injection shots indicates that core region electron thermal convection losses

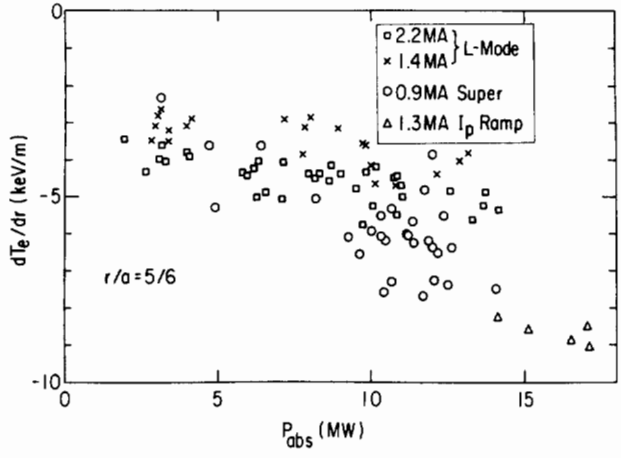

FIG. 5. Edge temperature gradient versus absorbed beam power for the same data sets as in Fig. 1.

$(5/2r_eT_e)$ are comparable to electron conduction losses at the end of injection. The argument that an effect of this magnitude is adequate to alter $T_e(r)$ in the core is bolstered by the observation that an even stronger central flattening of T_e is seen early in the injection pulse (t = 4.15 sec in Fig. 4), when the rapid build-up of central density results in a dW_e/dt term which is also comparable to conduction, but over a larger region. Furthermore, when the cold electron source is turned off at the end of injection, the central electron temperature rises (t = 4.6 sec in Fig. 4), and the profile shape regains the characteristic central peak of a high-q ohmic discharge. (Issues associated with the Δ' stability of these discharges are discussed in [3]).

If the electron temperature profile in the bulk of the minor radius in supershots is controlled by a mechanism of profile consistency such as transport coefficeients which depend strongly on $\nabla T_e/T_e$, and the core region is possibly clamped by convective losses, then we should look to the outer region for the enhanced confinement properties of supershots. Figure 5 shows dT_e/dr at r = 5a/6 versus absorbed power for the data set of Fig. 1. As expected for consistency with L-mode current scaling, the 1.4 MA shots show a lower edge temperature gradient than the 2.2 MA shots. However at high power the 0.9 MA supershots have a steeper outer region temperature gradient than even the 2.2 MA shots. On the basis of L-mode scaling, and profile consistency, these gradients would normally be expected to vary inversely with density, since in the L-Mode W_e is found to depend only weakly on $\bar{n}_e$. In the power range of $P_{inj} > 10$ MW, the 2.2 MA discharges in this data set have $\bar{n}_e \approx 4.4 \times 10^{19} m^{-3}$, the 1.4 MA shots and the current ramp shots both have $\bar{n}_e \approx 3.4 \times 10^{19} m^{-3}$, while the 0.9 MA supershots have $\bar{n}_e \approx 2.7 \times 10^{19} m^{-3}$. The lower line average

density of the supershots is therefore not adequate to explain their steeper edge gradients. This suggests that the reduced recycling coefficient of the degassed limiters, coupled with deep beam fueling, permits a low edge density and less convective losses in the enhanced confinement regime, giving rise to a hotter edge. Absolute Dα measurements, coupled with neutral modeling calculation, indicate τ_p of the order of 30 msec for the gas-filled limiter case shown in Figure 4 of [1], and dT_e/dr at 5a/6 in that case is only 3.5 keV/m. Transport analysis of this discharge indicates that at the edge of the plasma convective losses dominate conduction in the electron power balance (as in high recycling conditions in D-III [7]), explaining the low edge electron temperature and, through the constraint of profile consistency, perhaps the overall reduction in confinement.

4. The Electron Density Profile

The peaked density profiles observed in the enhanced confinement regime appear to be the result of a beam build-up instability [8]. In the discharge illustrated in figure 4, at 0.1 sec into the beam pulse transport analysis calculations indicate that $n_b(0)/n_e(0) \approx 0.4$, and the beam density is strongly peaked on axis, contributing most of the core density gradient. As the beam ions slow down the background density builds up, and at the end of the beam pulse $n_b(0)/n_e(0)$ has dropped to ≈ 0.2. The central electron density rises at about 70% of the beam fueling rate for the first 0.3 sec of injection, and later rises at 20-30% of the source rate. The importance of central beam deposition to this build-up process may explain the sensitivity of the supershot mode to plasma current. The minimum attainable initial target density in cases with a well-degassed limiter is observed to be proportional to $I_p^{1.5}$ in the range of 0.8-1.2 MA, and the Shafranov shift drops rapidly as a function of current, so that $\int ndl$ between the edge and the plasma core increases strongly with I_p. The shift may be especially important, because the tightly compressed outer flux surfaces present a thin target to neutral beam injection, and particles deposited in that region are distributed around the volume of the flux surface, which is largely hidden from the beam by the plasma core. Spectroscopic measurements also indicate higher carbon influx rates at higher currents. This further helps to explain the absence of peaked density profiles and supershot behavior at high current. L-Mode and ohmically heated plasmas generally have more peaked density profiles at $q_a > 5$ as well, suggesting an increased susceptibility to this process at high q_a.

There are a number of ways in which a peaked density profile can mediate improved confinement. One natural hypothesis is that the peaked profiles reduce η_i and/or η_e which could be important factors in the instabilities which drive transport ($\eta_{i,e} \equiv d\ell nT_{i,e}/d\ell nn_{i,e}$). η_i has not been measured on TFTR, but η_e can be calculated from the Thomson scattering data. In the

region inside 0.4a n_e is significantly lower in supershots than in standard discharges, dropping at high powers from values in the range of 1.7 at 0.4a for standard discharges to 1.2 in the enhanced confinement mode. An alternative hypothesis discussed in section 3 above, is that high edge electron temperatures, in the presence of reduced recycling and low edge densities, may result in relatively low values for edge transport coefficients as in the H-mode. In the presence of even constant edge transport coefficients, electron temperature profile consistency arguments which take into consideration the presence of a centrally peaked density profile, but assume that the edge electron thermal diffusivity responds only to the local n_e, predict a significant improvement in W_e [9].

5. Balanced vs. Unbalanced Injection and Plasma Rotation

As indicated in [1], the stored energy in supershot plasmas shows a considerable improvement as the beam powers in the co and counter directions are brought into balance. Because of the present configuration of TFTR (3 co-beamlines and 1 counter-beamline for the usual direction of I_p) we have not obtained high power data with pure counter-injection and a well-degassed limiter. At low currents (600-800 kA), however, enhanced confinement discharges with favorable time evolution and highly peaked density profiles can be obtained with only 5 MW of balanced injection power, and the full spectrum of P_{co}/P_{inj} can be explored. We find that the density increase at fixed injection power drops with rising P_{co}/P_{inj}, but the peakedness of the density profile falls off as one moves away from balanced injection in either direction. Stored energy and especially neutron production fall off as well. Plasma rotation speeds of $\approx 8 \times 10^5$ m/sec have been measured in co-injected discharges, corresponding to a Mach number of ≈ 0.7. Rotation speeds with counter-injection are lower than with co-injection at the same power.

A number of classically expected factors may lead to reduced density peaking and poorer heating efficiency at high rotation speeds with unidirectional injection [10]. In the rotating plasma frame the beam ions, and especially the fractional energy component beam ions (which constitute about one half of the total beam), have considerably reduced energy. This results in larger atomic cross-sections for beam deposition and a larger fraction of the deposition on hydrogenic species in the form of charge-exchange rather than impact ionization. Because of the lower beam ion velocity in the plasma frame, the beam ion slowing down time and therefore the beam ion density is substantially reduced. In an extreme example (13 MW of co-injection at $I_p = 0.9$ MA with $v_\phi(0) = 7.5 \times 10^5$ m/sec) taking these effects into account in somewhat simplified calculations results in a 30% reduction of central electron source rate. The central beam ion density at the end of injection is reduced by a factor of 3. If the presence of

a central peak of circulating beam ions is important for establishing a sharp electron density profile, it is reasonable to expect that this sharpness will be reduced in a rapidly rotating plasma. At the high Mach numbers we have observed, one expects significant centrifuging of plasma density, and especially of impurity density, to the large major radius side of the plasma. Thomson scattering measurements show a definite trend in this direction, correlated with unbalanced injection. Detailed scaling studies have not been made, but effects of the magnitude expected are observed. This centrifuge effect should tend to reduce beam penetration to the center of the plasma. To determine whether these classically expected effects of rotation are enough to explain the differences in the density profiles we observe, without additional changes in central particle diffusivity, will require more detailed calculations and examination of the data. The increased density rise in counter-injected discharges almost certainly also plays a role in the broad density profiles observed in the more slowly rotating counter-injected plasmas.

Lower beam velocity in the plasma frame results in a strong reduction in the beam-target and beam-beam fusion neutron yield; unidirectional injection reduces beam-beam neutron production as well. In the example above the effects of plasma rotation reduce the calculated neutron flux by a factor of 2, and good agreement is obtained with the measurement. The importance of plasma rotation for neutron production is most clearly illustrated by the rapid rise in neutron production observed when a low-current plasma is first heated with 5 MW of co-only injection, and then the co beams are switched off and 5 MW of counter beams turned on. The neutron emission rises by a factor of 2 in 50 msec.

With unbalanced injection a substantial fraction of the beam power is invested in applying torque to the rotating plasma. Much of this power is expected to be returned to the bulk ions via viscous damping mechanisms in the region where the gradients in rotation speed are high, probably close to the plasma surface. In this region ion thermal losses through convection and charge-exchange are large however. Rotational energy may also be partially lost from the plasma via the same mechanisms. In the example discussed above, this process, plus the reduction in beam penetration, results in a 50% reduction of central heating power, and an overall 40% investment of beam heating power in driving rotation. If the power is not coupled back to the plasma, the lower total stored energy observed with co-only injection [1] is reasonably well explained. Central ion temperature measurements in co-only cases are also reduced compared to balanced injection with similar parameters, consistent with the calculated reduced central input power to the ions. Rotational energy is probably coupled back into the bulk thermal plasma with some efficiency, and it is thus a mix of this mechanism and the broader density profiles observed with co-only injection which together result in reduced stored energy.

6. Conclusions

A new mode of enhanced energy confinement has been observed on TFTR. It exhibits improved electron stored energy, as well as improved thermal and beam ion stored energy. The broad electron temperature profile shapes observed in this regime at high q_a do not support a concept of profile consistency based on the assumption that $T_e(0)/\langle T_e \rangle_v = f(q_a)$, but do fit with a model based on examining normalized profile shapes outside of the plasma core, independent of q_a [6, 11]. The observation that increased recycling results in a convection-dominated edge electron power balance, which then correlates with reduced overall confinement, fits well with an understanding of this regime based on profile consistency arguments [9]. On the other hand it is also a reasonable hypothesis that the reduction of n_e and/or n_i in the core region plays an important role.

The peaked density profiles observed in this regime appear to be due to a beam build-up process which results in highly centralized beam deposition. Density profiles are most peaked with near-balanced injection, and some classically expected mechanisms have been put forward to explain this, but it is not clear whether other effects are required. Neutron production and beam heating efficiency are also highest with near-balanced injection. Classical calculations including plasma rotation are adequate to explain the difference in neutron production rate with co-only and balanced injection, given the differences in plasma profiles. The fractional power delivered to the plasma in the form of torque on a rotating body is comparable to the fractional difference in stored energy between co-only and balanced injection. Some of this power, however, is probably re-invested in ion heating near the outside in minor radius. The combination of the resulting reduction in heating efficiency and the broader density profiles observed with unbalanced injection together explain the importance of balanced injection for obtaining the best results in the TFTR "supershot" regime.

ACKNOWLEDGMENTS

We are grateful to D.J. Grove and J.R. Thompson for their advice and support, and to J. Strachan for his many contributions. This work was supported by US DOE Contract No. DE-AC02-76-CH03073. The ORNL participants were also supported by U.S. Department of Energy Contract No. DE-AC05-84OR21400 with Martin Marietta Energy Systems, Inc.

REFERENCES

[1] HAWRYLUK, R.J., et al., Paper IAEA-CN-47/A-I-3, these Proceedings, Vol. 1.
[2] HILL, K.W., et al., Paper IAEA-CN-47/A-IV-2, these Proceedings, Vol. 1.
[3] McGUIRE, K., et al., Paper IAEA-CN-47/A-VII-4, these Proceedings, Vol. 1.

[4] GOLDSTON, R.J., Plasma Phys. Control. Fusion **26** (1984) 87.
[5] WALTZ, R.E., Comments on Profile Consistency, Rep. GAT-A 18365, Goodyear Atomic Corp., Portsmouth, OH.
[6] FREDRICKSON, E., et al., in Controlled Fusion and Plasma Heating (Proc. 13th Europ. Conf. Schliersee, 1986), Vol. 1, European Physical Society (1986) 148.
[7] NAGAMI, M., et al., Nucl. Fusion **24** (1984) 183.
[8] POST, D.E., private communication, 1978.
[9] FURTH, H.P., Plasma Phys. Controll. Fusion **28** (1986) 1305.
[10] GOLDSTON, R.J., in Basic Physical Processes of Toroidal Fusion Plasmas (Proc. Course and Workshop Varenna, 1985), Vol. 1, EUR-10418-EN, CEC, Brussels (1986) 165*.
[11] MURMANN, H.D., et al., in Controlled Fusion and Plasma Heating (Proc. 13th Europ. Conf. Schliersee, 1986), Vol. 1, European Physical Society (1986) 216.

DISCUSSION

A. BHATTACHARJEE: I have a comment and a question. In the presence of toroidal rotation, the density on any given flux surface becomes poloidally asymmetric. This, as you know, was observed in PDX. However, the magnitude of toroidal rotation necessary to explain the asymmetry experimentally observed was found to be greater than the rotation actually observed, for example, by S. Semenzato et al. at the Centre de recherches en physique de plasmas, Lausanne. It appears that the same could be said of TFTR.

My question is: why is it that the rotation velocity observed is different for co-injection and counter-injection when the beam power is held fixed?

R.J. GOLDSTON: On TFTR, as on PDX, we do see some in–out asymmetry in the Thomson scattering density profiles, even in Ohmic plasmas. We have found, however, that there is a systematic further asymmetry which correlates with unbalanced injection. The degree of this further asymmetry is roughly in agreement with what would be theoretically expected, but we have not yet carried out detailed scaling studies on the asymmetry.

Counter-injection does indeed drive less central rotation speed than co-injection, for fixed power, but the density is higher. We have not yet measured the radial profile of the rotation, so I am hesitant to suggest an explanation.

B. COPPI: I should just like to comment that the lack of dependence of $T_e(0)/T\langle T_e\rangle_{av}$ on q_a when $q(r = 0) > 1$ was in fact pointed out in the original formulation for the principle of profile consistency. Therefore, the observations you

---

* The last term in Eq. (26) of this reference should read:

$$+ \frac{\Sigma m_i \omega^2}{2} \left(\frac{\partial V}{\partial \rho}\right)^{-1} \left\{\frac{\partial}{\partial \rho}\left[\langle R^2 (\vec{\nabla}\rho)^2\rangle \left(\frac{\partial V}{\partial \rho}\right) n_i \left(\frac{\vec{v}}{\vec{\nabla}\rho}\right)\right]\right.$$
$$\left. - \langle R^2\rangle \frac{\partial}{\partial \rho}\left[\langle (\vec{\nabla}\rho)^2\rangle \left(\frac{\partial V}{\partial \rho}\right) n_i \left(\frac{\vec{v}}{\vec{\nabla}\rho}\right)\right]\right\}$$

reported do not require a reformulation of this principle. In addition, the temperature profile may deviate considerably from a Gaussian, depending on a variety of factors, for example, the presence of trapped electrons, under the same formulation.

R.J. GOLDSTON: Thank you for the comment.

A. GIBSON: Now that you have the concept of profile consistency with so many 'ifs' and 'buts' and restricted it to such a special region of the profile, do you still believe it has any physical significance, and if so what is it?

R.J. GOLDSTON: Researchers have frequently divided the tokamak into three zones — a central sawtoothing zone, a middle 'confinement' zone, and an edge zone dominated by convection and atomic physics. The refinement we proposed at the 13th European Conference in 1986 and which we are discussing here is that the resiliency of the profile applies mostly in the middle 'confinement' zone. Lower hybrid heating experiments certainly show that the presence or absence of sawteeth can strongly attack the core zone, and the H-mode is an example of how the edge can be modified. The fact that modifications of the edge region can have profound effects on core transport strongly suggests a transport mechanism which resists profile shape changes. One example would be a model which includes ∇T_e or $d \ln T_e/dr$ in the electron thermal diffusivity itself.